Alexandria Engineering Journal (2022) 61, 9811–9818

HOSTED BY

ELSEVIER

Alexandria University

Alexandria Engineering Journal

www.elsevier.com/locate/aej
www.sciencedirect.com

# An experimental study of the air-side performance of a novel louver spiral fin-and-tube heat exchanger

**Parinya Kiatpachai [a], Thawatchai Keawkamrop [a], Lazarus Godson Asirvatham [b], Mehrdad Mesgarpour [a], Ahmet Selim Dalkılıç [c], Ho Seon Ahn [d], Omid Mahian [e,f], Somchai Wongwises [a,g,*]**

[a] *Fluid Mechanics, Thermal Engineering and Multiphase Flow Research Lab (FUTURE), Department of Mechanical Engineering, Faculty of Engineering, King Mongkut's University of Technology Thonburi (KMUTT), Bangkok 10140, Thailand*
[b] *Department of Mechanical Engineering, Karunya Institute of Technology and Sciences, Coimbatore, Tamil Nadu, India*
[c] *Department of Mechanical Engineering, Yildiz Technical University, Yildiz, Besiktas, Istanbul, Turkey*
[d] *Department of Mechanical Engineering, Incheon National University, Incheon, Republic of Korea*
[e] *School of Chemical Engineering and Technology, Xi'an Jiaotong University, Xi'an, China*
[f] *Department of Mechanical Engineering, Center for Nanotechnology in Renewable Energies, Ferdowsi University of Mashhad, Mashhad, Iran*
[g] *National Science and Technology Development Agency (NSTDA), Pathum Thani 12120, Thailand*

Received 21 August 2021; revised 30 January 2022; accepted 23 February 2022
Available online 07 March 2022

**KEYWORDS**

Heat exchanger;
Spiral fin;
Louver fin;
Spiral fin and tube heat exchanger

**Abstract** We studied the effect of fin patterns on the air-side performance of a novel type of heat exchanger, namely louver spiral fin-and-tube heat exchangers (LSFTHXs). We investigated three types of fin patterns—radial, curved, and mixed-louver spiral fins—and compared their characteristics with plain spiral fin. We fabricated heat exchangers with a crimped aluminum fin base, two rows of steel tubes, and a fin pitch of 8.45 mm. All heat exchangers had both multipass parallel and counter cross-flow arrangements. The average heat transfer rate ($Q_{ave}$), heat transfer coefficient ($h_o$), and pressure drop ($\Delta P$) increased along with frontal air velocity. The louver-spiral fin provided greater $Q_{ave}$ and $h_o$ than plain-spiral fin by about 9.7–15.6% and 13.4–27.1%, respectively. The $j$ factors (Colburn factors) of louver-spiral fins were greater by approximately 10.4–13.1% (for mixed LSFTHX), 7.7–8.8% (for radial LSFTHX), and 2.1–5.1% (for curved LSFTHX) compared with the plain SFTHXs. Additionally, we found no significant difference in $\Delta P$ or f factor (friction factor) between louver-spiral and plain-spiral fins. LSFTHX configurations increased $h_o$ and $j$.



* Corresponding author at: Fluid Mechanics, Thermal Engineering and Multiphase Flow Research Lab (FUTURE), Department of Mechanical Engineering, Faculty of Engineering, King Mongkut's University of Technology Thonburi (KMUTT), Bangkok 10140, Thailand.
E-mail address: somchai.won@kmutt.ac.th (S. Wongwises).

Peer review under responsibility of Faculty of Engineering, Alexandria University.

https://doi.org/10.1016/j.aej.2022.02.056

## 1. Introduction

The most productive studies dealing with spiral fin-and-tube heat exchangers (SFTHXs) were conducted by the following researchers:

Srisawad and Wongwises [1] studied crimped spiral fin-and-tube heat exchangers (CSFTHXs). The air-side performance (ASP) of the heat exchangers was investigated under dry and wet surface conditions, along with various temperature, air velocity, flow rate and air humidity conditions. Lee et al. [2] clarified the effect of conventional SFTHXs' fin patterns on ASP. The effects of fin pitch ($f_p$), number of tube rows ($N_{row}$), and fin alignment were investigated in terms of $j$ factor (Colburn factor) and $f$ factor (friction factor). Those parameters were used to evaluate optimal ASP. Pongsoi et al. [3] studied the effect of $f_p$ (3.2, 4.2, 6.2 mm) and fin materials (copper and aluminum) on the CSFTHXs' ASP. $f_p$ and fin material had significant effect on $Q_{ave}$, $\Delta P$, and fin efficiency ($\eta_f$). Pongsoi et al. [4] reported the effect of $N_{row}$ on CSFTHXs' ASP, showing that $Q_{ave}$ and $\Delta P$ increased along with $N_{row}$. To optimize $f_p$, Pongsoi et al. [5] used the three performance indexes to study the effect of $f_p$ on optimal ASP for CFSTHXs. Their analysis showed that one of the proposed indexes could be applied at an $f_p$ of 4.2 mm for optimal design in industrial applications.

Pongsoi et al. [6] tested the ASP of an L-footed SFTHX. Their results confirmed that $N_{row}$ (2, 3, or 4), fin outside diameter (30.5 and 35.0 mm), and fin materials significantly affected $Q_{ave}$, $\Delta P$, and $\eta_f$. However, $N_{row}$ had no significant effect on ASP ($j$ and $f$ factors). Pongsoi et al. [7] clarified the ASP of L-footed SFTHXs with variations of $f_p$ from 2.4 to 4.2 mm. $f_p$ had a significant effect on $f$ at $Re_{dc}$ of 6,000–15,000. In contrast, $f_p$ had a negligible effect on $j$ for L-footed SFTHXs. Pongsoi et al. [8] also reviewed and summarized articles concerning SFTHX. They briefly described SFTHX and circular FTHX. They also compared ASP values for several spiral fin types. Correlations for the ASP of L-footed, crimped, conventional, and serrated fins were compiled by Pongsoi et al. [8]. Pongsoi and Wongwises [9] used the performance index to analyze ASP at various fin pitches of L-footed SFTHXs. They found that an $f_p$ of 2.4 and 3.2 mm of L-footed SFTHX at a high Reynolds number were an optimal configuration for HX design. Kiatpachai et al. [10] investigated the ASP of serrated SFTHXs with various $f_p$ values of 3.6 to 6.2 mm. $Q_{ave}$ and $\Delta P$ increased along with $f_p$. However, the effect of $f_p$ on the air-side heat transfer coefficient ($h_o$) was very small. Zhou et al. [11] tested serrated and twisted-serrated SFTHXs to compare their ASP in terms of $j$, $f$, and Nusselt number ($Nu$). The twisted-serrated SFTHX exhibited greater $h_o$ and $\Delta P$ values. Keawkamrop et al. [12] studied the effects of $f_p$ and fin height on the CSFTHXs' ASPs using a small tube diameter of 9.53 mm. Additionally, they proposed the correlations of $Nu$, $j$, and $f$ for designing SFTHXs used in thermal industries.

According to the literature, several SFTHX types have been studied for applications in thermal processes: helically coiled CSFTHX [1], conventional SFTHX [2], CSFTHX [3–5,12], L-footed SFTHX [6–7,9], serrated SFTHX [10–11], and several SFTHXs [8]. These researchers created innovations for new thermal equipment. Among several types of SFTHXs, CFTHXs have received special attention. Tang et al. [13] confirmed that CSFTHXs yielded greater ASP than other FTHX types. Additionally, the effect of the louver fin shape on the ASP of the plate FTHX was studied by [14], who confirmed that louver fins enhanced heat transfer.

The information above led us to the idea to combine a crimped-spiral fin with a louver-spiral fin, which could lead to a new kind of SFTHX. Until now, there has been only one work dealing with louver-spiral-finned tubes [15]. However, although some information is currently available, no detailed investigation exists. In this study, we present the effects of louver fin patterns on the ASP values of LSFTHXs with crimped fin bases, information that has never been published. We tested radial-, curved-, and mixed-louver SFTHXs, as well as plain SFTHXs with two rows and a fin pitch of 8.45 mm. All experiments were done at a high Reynolds number.

## 2. Experimental apparatus and procedure

The experimental apparatus shown in Fig. 1 consists of the test sections and a wind tunnel. The four test sections were the mixed, radial, and curved LSFTHXs, and a plain SFTHX with a crimped-fin base, two rows, z-shaped tube arrangement, and a fin pitch of 8.45 mm. The details of the heat exchanger can be seen in Table 1. Hot water and ambient air were used as working fluids. The experimental conditions for various parameters (air frontal velocity ($V_{fr}$), Reynolds number based on tube outside diameter ($Re_{do}$), inlet water temperature ($T_{w,in}$), and water mass flow rate ($m_{w,in}$)) are shown in Table 2. The accuracy of the measurements is shown in Table 3. More detailed information can be found in [5].

Fig. 2 shows the photos of mixed, radial, and curved LSFTHXs, and the plain SFTHX used in our study. LSFTHX dimensions and flow arrangements are shown in Fig. 3.

## 3. Data reduction

We calculated the overall heat transfer coefficient ($U$) using Eq. (1).

$$\frac{1}{UA} = \frac{1}{h_i A_i} + \frac{\ln(d_o/d_i)}{2\pi k_t L} + \frac{1}{\eta_o h_o A_o} \tag{1}$$

where $A$ is surface area, $h_i$ and $h_o$ are tube-side and air-side heat transfer coefficients, respectively, $A_i$ and $A_o$ are inner tube surface area and total surface area, respectively, $d_i$ and $d_o$ are tube inside and tube outside diameters, respectively $k_t$ = thermal conductivity of tube, $L$ = length of heat exchanger, $\eta_o$ = overall surface effectiveness

The effectiveness (ε) for the multipass parallel cross flow (MPCF) (Eq. (2)) and the multipass counter cross flow (MCCF) (Eq. (3)) were combined for z-shape tube arrangement.

For MPCF with $N_{row}$ = 2:

$$\varepsilon_c = 1 - \left[\frac{K}{2} + \left(1 - \frac{K}{2}\right)e^{2K/C_A^*}\right]^{-1}, \quad K = 1 - e^{-NTU_A(C_A^*/2)} \tag{2}$$

where $\varepsilon_c$ is heat exchanger effectiveness for MCCF, $C^*$ = capacity rate ratio, NTU = number of transfer units

For MCCF with $N_{row}$ = 2:

$$\varepsilon_p = \left(1 - \frac{K}{2}\right)\left(1 - e^{-2K/C_A^*}\right), \quad K = 1 - e^{-NTU_A(C_A^*/2)} \tag{3}$$

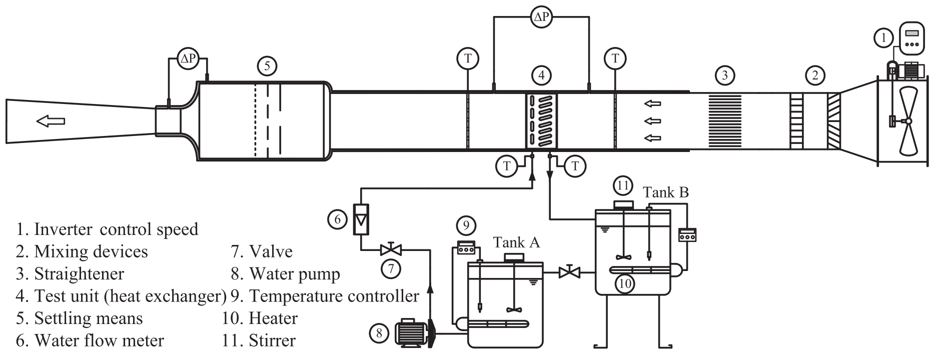


**Fig. 1** Schematic diagram of the apparatus [From [7], with permission from Elsevier].

**Table 1** Geometric parameters of the LSFTHXs with crimped fin base.

| No. | Spiral fin patterns | $d_i$ | $d_o$ | $d_f$ | $P_L$ | $P_T$ | $f_t$ | $n_t$ | $N_{row}$ | $f_p$ | Fin material | Tube material |
|---|---|---|---|---|---|---|---|---|---|---|---|---|
| 1 | Mixed louver | 27.2 | 34 | 61.5 | 79 | 66 | 1 | 4 | 2 | 8.45 | Aluminum | Steel |
| 2 | Radial louver | 27.2 | 34 | 61.5 | 79 | 66 | 1 | 4 | 2 | 8.45 | Aluminum | Steel |
| 3 | Curved louver | 27.2 | 34 | 61.5 | 79 | 66 | 1 | 4 | 2 | 8.45 | Aluminum | Steel |
| 4 | Plain | 27.2 | 34 | 61.5 | 79 | 66 | 1 | 4 | 2 | 8.45 | Aluminum | Steel |

Note: Dimensions in mm.

**Table 2** Test conditions.

| | |
|---|---|
| Temperature of inlet air, °$C$ | 31.5 ± 0.5 |
| Frontal velocity of inlet air, $m/s$ | 2–7 or $Re_{do}$ (7,000–25,000) |
| Temperature of inlet water, °$C$ | 60–70 |
| Flow rate of water, $kg/s$ | 0.167–0.233 |

**Table 3** Accuracy of measurements.

| Parameters | Accuracy |
|---|---|
| Temperature of inlet air, °$C$ | ±0.1 |
| Pressure drop, $Pa$ | ±0.5 |
| Temperature of inlet water, °$C$ | ±0.1 |
| Flow rate of water, $kg/s$ | ±0.4 (±0.02 of full scale) |

where $\varepsilon_p$ is heat exchanger effectiveness for MPCF, $C^* = C_{min}/C_{max}$ is the relative magnitudes of the cold and hot fluid heat capacity rates.

We used a multipass parallel and counter cross-flow (MPCCF) arrangement—a combination of both flow configurations—to determine their average effectiveness [6,16–18].

$$\varepsilon_{pc} = \frac{\varepsilon_P + \varepsilon_C}{2} \text{ for } N_{row} = 2 \tag{4}$$

Radial fin efficiency, one of Gardner's modified Bessel functions [19], was used to determine fin efficiency.

$$\eta_f = \frac{2\psi}{\varphi(1+\psi)} \frac{I_1(\varphi R_o)K_1(\varphi R_i) - I_1(\varphi R_i)K_1(\varphi R_o)}{I_0(\varphi R_i)K_1(\varphi R_o) + I_1(\varphi R_o)K_0(\varphi R_i)} \tag{5}$$

where

$$\varphi = (r_o - r_i)^{3/2}\left(\frac{2h_o}{k_f A_p}\right)^{1/2} \tag{6}$$

where $\eta_f$ is fin efficiency, $\psi$ is radius ratio, $\varphi$ is combination of terms, $I_0$ and $I_1$ = modified Bessel function solution of the first kind order 0 and order 1, respectively, $K_0$ and $K_1$ are modified Bessel function solution of the second kind order 0 and order 1, respectively, $R$ = radius function

Air-side heat transfer performance is presented in terms of the $j$ factor.

$$j = \frac{Nu}{Re_{do} Pr^{1/3}} = \frac{h_o}{\rho_a V_{\max} c_P}(Pr)^{2/3} \tag{7}$$

where $V_{max}$ is maximum velocity across heat exchanger.

$\Delta P$ across the heat exchanger is shown as friction factor [20].

$$f = \left(\frac{A_{min}}{A_o}\right)\left(\frac{\rho_m}{\rho_1}\right)\left[\frac{2\Delta P \rho_1}{G_c^2} - \left(1+\sigma^2\right)\left(\frac{\rho_1}{\rho_2} - 1\right)\right] \tag{8}$$

where $A_{min}$ is minimum free flow area, $\rho_m$ = average density of air, $\rho_1$ and $\rho_2$ are densities of air at inlet and outlet, respectively, $G_c$ = mass flux of the air at $A_{min}$, $\sigma$= contraction ratio of cross-sectional area

The average heat transfer rate is determined as $Q_{ave} = \frac{|Q_a|+|Q_w|}{2}$. Experiments were conducted based on ASHRAE standards [21], under which $|Q_a - Q_w|/Q_{ave}$ must be less than 0.05 (Fig. 4). For this study, the maximum uncertainties of $j$ and $f$ factors were 5.5 and 3.2%, respectively.

## 4. Results and discussion

This paper presents the effect of fin patterns on the ASP of LSFTHXs with a crimped-fin base and MPCCF arrangement. All heat exchangers had two rows and an $f_p$ of 8.45 mm. The

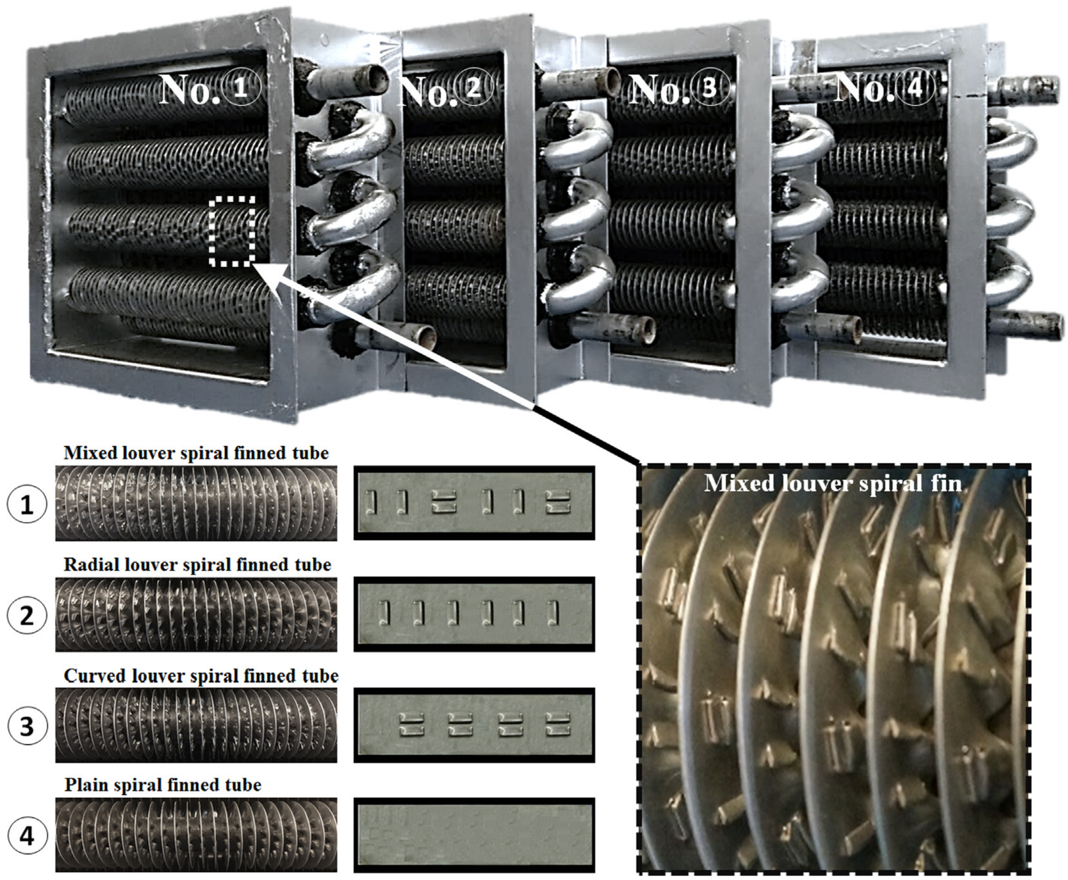


**Fig. 2** Mixed, radial and curved louver spiral fins, and plain spiral fin.

spiral-finned tube was fabricated from aluminum fin and copper tube. We focused on Reynolds numbers ranging from 7,000 to 25,000. Fig. 5(a) shows comparisons among several spiral fins and the effect of louver-spiral fin patterns on ASP in terms of $Q_{ave}$ based on varying $V_{fr}$. $Q_{ave}$ increased along with $V_{fr}$. Our results reveal that the louver-spiral fin yielded higher $Q_{ave}$ than plain-spiral fin by about 9.7–15.6%. This is because the total surface area ($A_o$) of the louver-spiral fin was greater than that of plain-spiral fin. The louver-fin pattern might also provide better mixing of air, leading to improved heat transfer performance.

Moreover, there was no significant difference in $Q_{ave}$ between mixed-, radial-, and curved-louver spiral-finned tubes. Fig. 5(b) presents an overview of $h_o$ by varying $V_{fr}$. Our results show that $h_o$ increases with greater $V_{fr}$. The effect of louver-spiral fin patterns was quite clear. Compared to plain-spiral fin, the $h_o$ of louver-spiral fin was greater by about 13.4–27.1%. The louver at the fin's surface generates good mixing of air and restarts the boundary layer, reducing total thermal resistances [14,22]. Fig. 5(c) shows the effect of the louver spiral fin patterns on $\Delta P$ at various $V_{fr}$ values. The $\Delta P$ increased as $V_{fr}$ increased, and the louver-spiral fin pattern had no significant effect on $\Delta P$. However, the $\Delta P$ obtained from the mixed, radial and curved LSFTHXs, and plain SFTHX were slightly different at $V_{fr}$ values of greater than 5 m/s. The performance index of louver-spiral fin calculated from $h_o/\Delta P$ was greater than that of plain-spiral fin.

The $j$ and $f$ factors shown in Eqs. (7) and (8) represent ASP for the dimensionless group. Figs. 6, 7, and 8 show the variations in $j$ and $f$ factors with $Re_{do}$ at various $T_{w,in}$ and $m_{w,in}$. For Fig. 6, the result confirms that $j$ and $f$ factors decrease as $Re_{do}$ increases from about 7,000–25,000. The correlations for $j$ and $f$ factors contained the main parameters; i.e., $Re_{do}$ (for $j$ in Eq. (7)), and $G_c$ (for $f$ in Eq. (8)). Both parameters were the denominators in Eqs. (7) and (8). Trends of the $j$ (and $f$) values obtained from various louver-spiral fin patterns with varia-

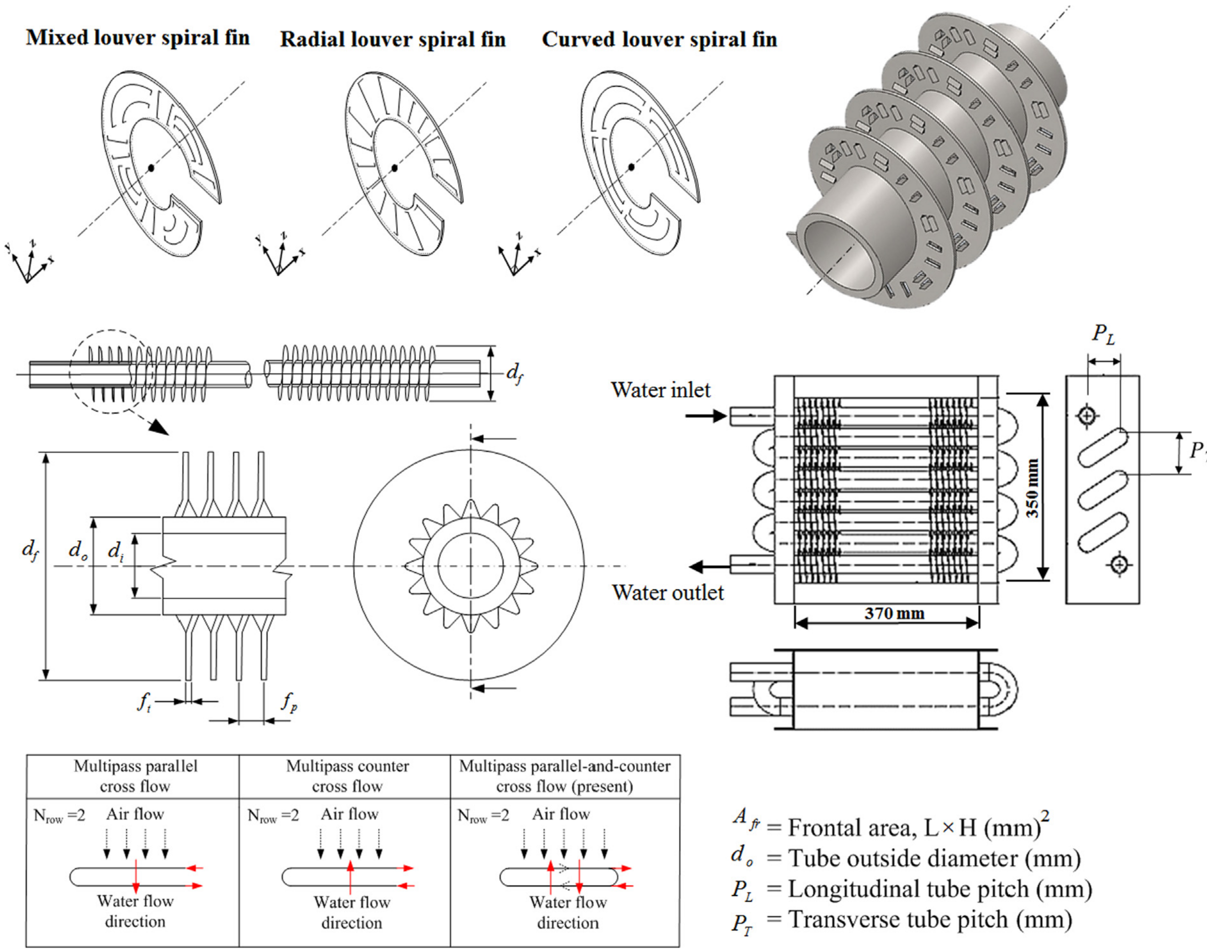


**Fig. 3** Geometric details of the LSFTHX using MPCCF.

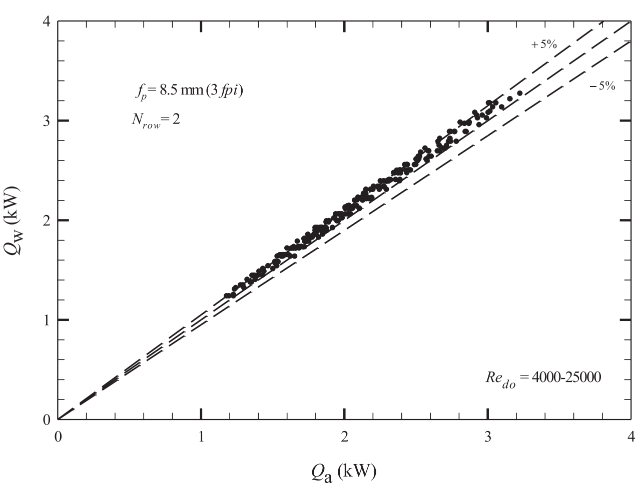


**Fig. 4** Energy balance between air and water.

tions of $Re_{do}$ were similar. The *j* factor decreased by up to 36.7% and the *f* factor decreases by up to 20.7% when $Re_{do}$ increased from about 7000–25,000. The *j* factors for mixed-, radial-, and curved-louver spiral fins were greater than 10.4–13.1%, 7.7–8.8%, and 2.1–5.1%, respectively, when compared with the plain-spiral fin. This was due to good mixing on the air side, which enhanced the LSFTHXs' performance. The mixed LSFTHX gave slightly greater $h_o$ and *j* factors than radial and curved LSFTHXs. However, the $\Delta P$ values obtained for all LSFTHXs were similar. The difference in the *f* values obtained from all the types of fins we tested was very little. This reflects that the louver-spiral fin pattern had no significant effect on *f*.

In Figs. 7 and 8, our results confirm that the variations of $T_{w,in}$ and $m_{w,in}$ still resulted in trends of *j* and *f* similar to those shown in Fig. 6.

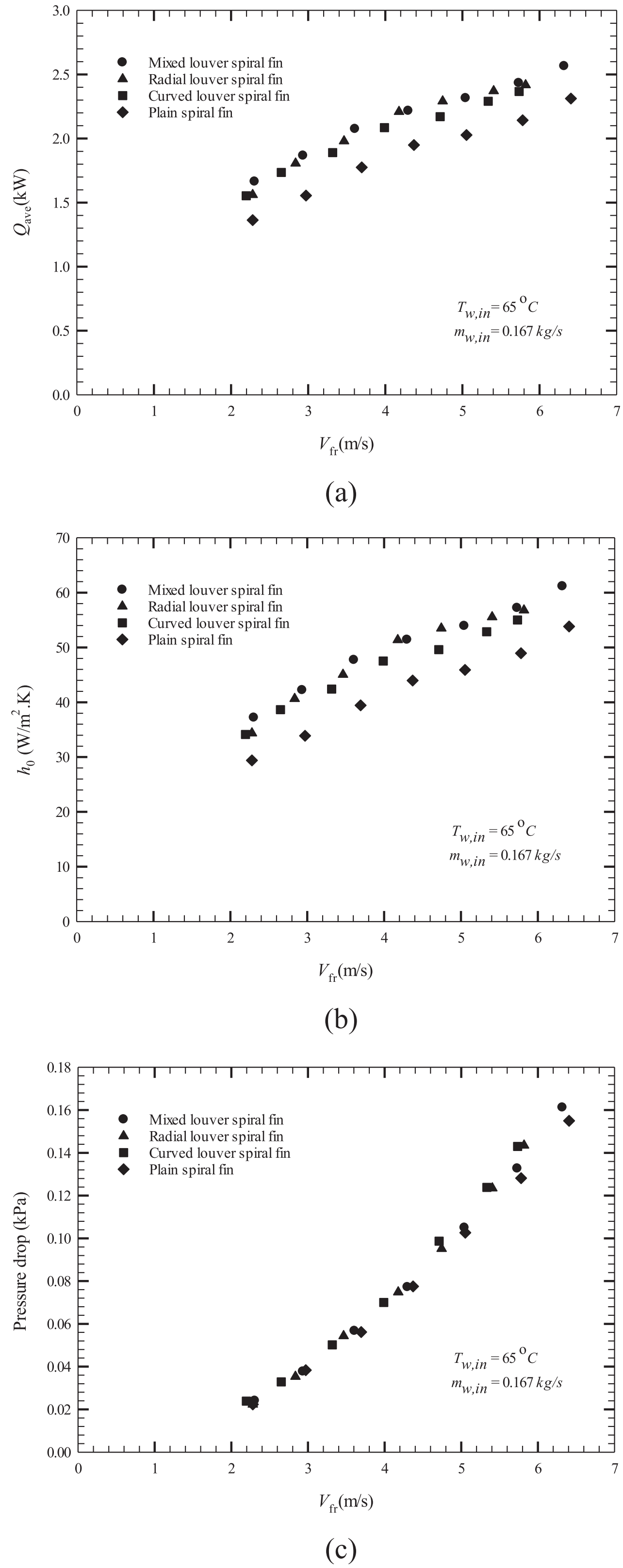


**Fig. 5** Effects of louver spiral fin patterns on (a) average heat transfer rate, (b) heat transfer coefficient, and (c) pressure drop of LSFTHXs.

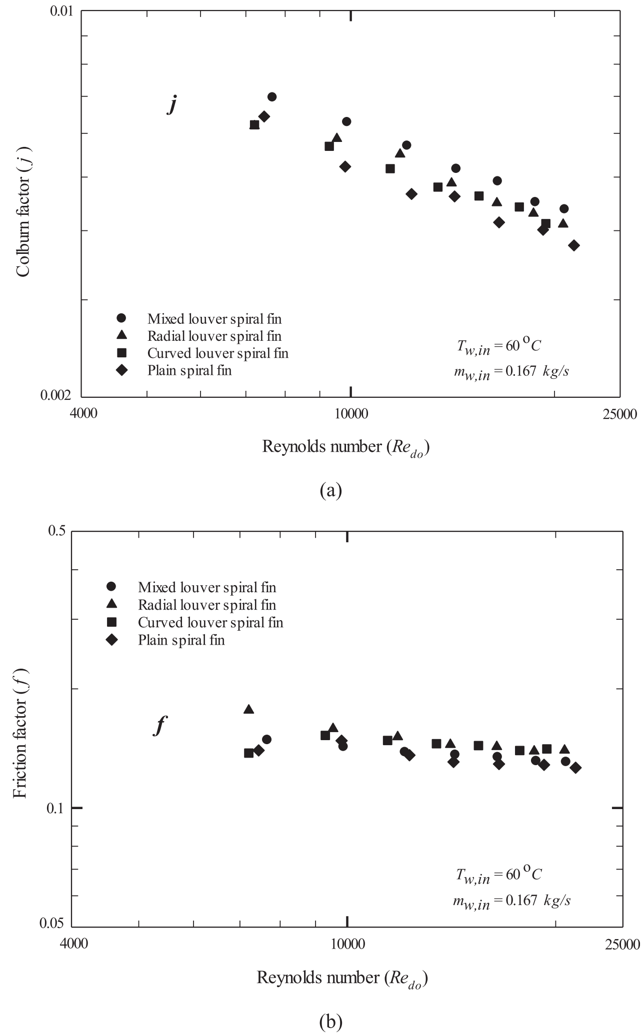


**Fig. 6** Effects of louver spiral fin patterns on (a) $j$ factor and (b) $f$ factor of LSFTHXs at $T_{w,in} = 60\ °C$ and $m_{w,in} = 0.167\ kg/s$.

## 5. Conclusion

We investigated LSFTHXs to study the effects of louver spiral fin patterns (mixed-, radial-, and curved-louver spiral fins and plain spiral fin) on ASP. The results of this investigation can be summarized as follows:

- Louver spiral fin patterns play a vital role in the performance of heat exchangers.
- The heat transfer rates and heat transfer coefficients of mixed-, radial-, and curved-louver spiral fins are greater than those of plain spiral fins by about 9.7–15.6% and 13.4–27.1%, respectively.
- The pressure drops and profiles obtained from mixed-, radial-, and curved-louver spiral fins and plain spiral fin were almost the same.
- Mixed-louver fins yielded the highest performance value in terms of Colburn factor compared to radial- and curved-louver spiral fins and plain spiral fin.
- Spiral-fin patterns had an insignificant effect on the friction factor.

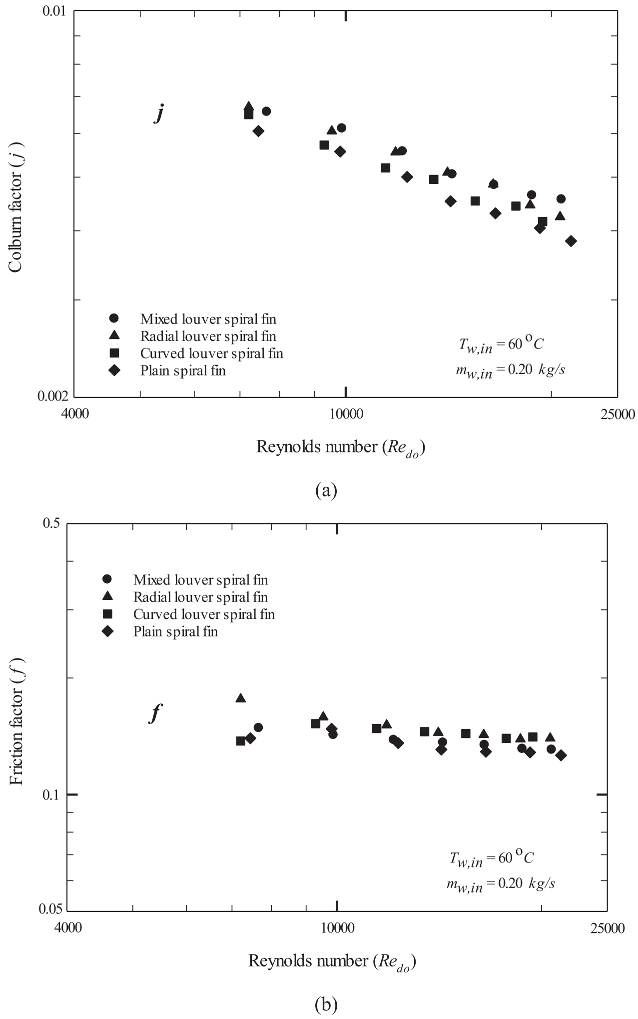


**Fig. 7** Effects of louver spiral fin patterns on (a) *j* factor and (b) *f* factor of LSFTHXs at $T_{w,in} = 60\ °C$ and $m_{w,in} = 0.2\ kg/s$.

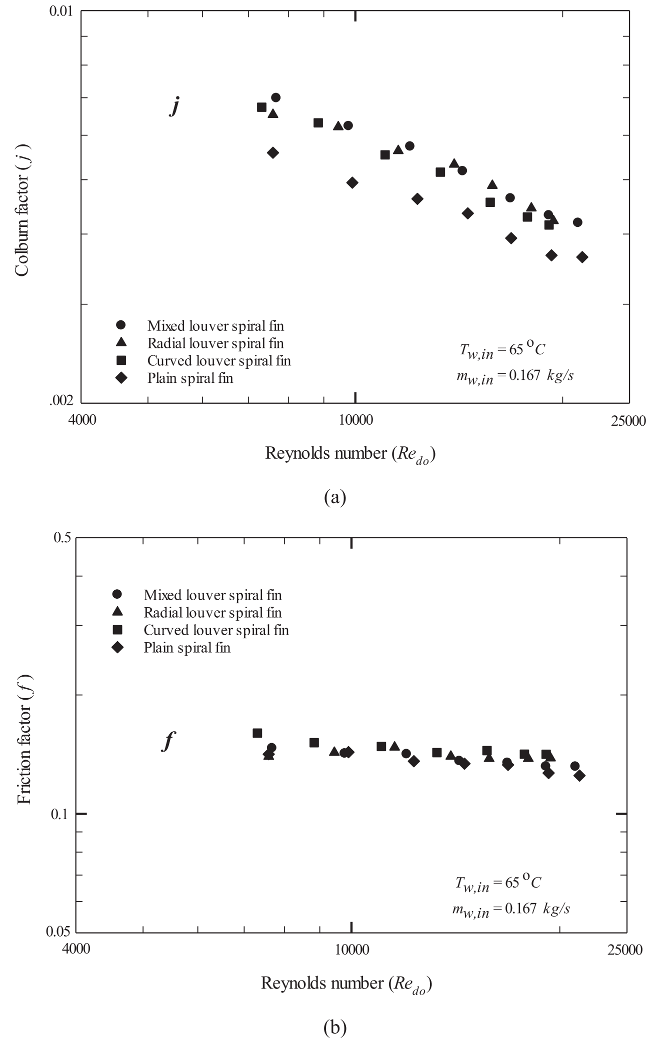


**Fig. 8** Effects of louver spiral fin patterns on (a) *j* factor and (b) *f* factor of LSFTHXs at $T_{w,in} = 65\ °C$ and $m_{w,in} = 0.167\ kg/s$.

## Declaration of Competing Interest

The authors declare that they have no known competing financial interests or personal relationships that could have appeared to influence the work reported in this paper.

## Acknowledgments

The second author acknowledges the Royal Golden Jubilee Ph.D. Program. The fourth author acknowledges the support of a Postdoctoral Fellowship from KMUTT. The authors acknowledge the Research Chair Grant provided by National Science and Technology Development Agency (NSTDA), and the Thailand Science Research and Innovation (TSRI) under Fundamental Fund 2022 (Project: Advanced Materials and Manufacturing for Applications in New S-curve Industries).

## References

[1] K. Srisawad, S. Wongwises, Heat transfer characteristics of a new helically coiled crimped spiral finned tube heat exchanger, Heat Mass Transfer 45 (4) (2009) 381–391.
[2] M. Lee, T. Kang, Y. Kim, Air-side heat transfer characteristics of spiral-type circular fin-and-tube heat exchangers, Int. J. Refrig. 33 (2010) 313–320.
[3] P. Pongsoi, S. Pikulkajorn, C.C. Wang, S. Wongwises, Effect of fin pitches on the air-side performance of crimped spiral fin-and-tube heat exchangers with a multipass parallel and counter cross-flow configuration, Int. J. Heat Mass Transfer 54 (9–10) (2011) 2234–2240.
[4] P. Pongsoi, S. Pikulkajorn, C.C. Wang, S. Wongwises, Effect of number of tube rows on the air-side performance of crimped spiral fin-and-tube heat exchangers with a multipass parallel and counter cross-flow configuration, Int. J. Heat Mass Transfer 55 (2012) 1403–1411.
[5] P. Pongsoi, S. Pikulkajorn, S. Wongwises, Effect of fin pitches on the optimum heat transfer performance of crimped spiral fin-and-tube heat exchangers, Int. J. Heat Mass Transfer 55 (23-24) (2012) 6555–6566.
[6] P. Pongsoi, S. Pikulkajorn, S. Wongwises, Experimental study on the air-side performance of a multipass parallel and counter cross-flow L-footed spiral fin and-tube heat exchanger, Heat Transfer Eng. 33 (15) (2012) 1251–1263.
[7] P. Pongsoi, P. Promoppatum, S. Pikulkajorn, S. Wongwises, Effect of fin pitches on the air-side performance of L-footed spiral fin-and-tube heat exchangers, Int. J. Heat Mass Transfer 59 (2013) 75–82.
[8] P. Pongsoi, S. Pikulkajorn, S. Wongwises, Heat transfer and flow characteristics of spiral fin-and-tube heat exchangers: A review, Int. J. Heat Mass Transfer 79 (2014) 417–431.
[9] P. Pongsoi, S. Wongwises, Determination of fin pitches for maximum performance index of L-footed spiral fin-and-tube heat exchangers, J. Therm. Eng. 1 (1) (2015) 251–262.
[10] P. Kiatpachai, S. Pikulkajorn, S. Wongwises, Air-side performance of serrated welded spiral fin- and-tube heat exchangers, Int. J. Heat Mass Transfer 89 (2015) 724–732.
[11] H. Zhou, D. Liu, Q. Sheng, M. Hu, Y. Cheng, K. Cen, Research on gas side performance of staggered fin-tube bundles with different serrated fin geometries, Int. J. Heat Mass Transfer 152 (2020) 119509.
[12] T. Keawkamrop, L.G. Asirvatham, A.S. Dalkılıç, H.S. Ahn, O. Mahian, S. Wongwises, An experimental investigation of the air-side performance of crimped spiral fin-and-tube heat exchangers with a small tube diameter, Int. J. Heat Mass Transfer 178 (2021) 121571.
[13] L.H. Tang, M. Zeng, Q.W. Wang, Experimental and numerical investigation on air-side performance of fin-and-tube heat exchangers with various fin patterns, Exp. Therm. Fluid Sci. 33 (5) (2009) 818–827.
[14] A. Sadeghianjahromi, S. Kheradmand, H. Nemati, J.S. Liaw, C. C. Wang, Compound Heat Transfer Enhancement of Wavy Fin-and-Tube Heat Exchangers through Boundary Layer Restarting and Swirled Flow, Energies 11 (8) (2018) 1959.
[15] S. Wongwises, P. Kiatpachai, US Patent No. US 10,436,524 B2, 2019.
[16] ESDU 86018, Effectiveness-NTU Relations for the Design and Performance Evaluation of two-stream heat exchangers, Engineering Science Data Unit 86018 with Amendment, London ESDU International PLC (1991) 92–107.
[17] H.A. Navarro, L. Cabezas-Gomez, A new approach for thermal performance calculation of cross-flow heat exchanger, Int. J. Heat Mass Transfer 48 (2005) 3880–3888.
[18] L. Cabezas-Gómez, J.M. Saiz-Jabardo, H.A. Navarro, P.E.L. Barbieri, New thermal effectiveness data and formulae for some cross-flow arrangements of practical interest, Int. J. Heat Mass Transfer 69 (2014) 237–246.
[19] K.A. Gardner, Efficient of Extended Surface, ASME Trans. 67 (1945) 621.
[20] W.M. Kays, A. London, Compact heat exchangers, third ed., Mcgraw-Hill, New York, 1984.
[21] ANSI/ASHRAE Standard 33-2000, Method of Testing Forced Circulation Air Cooling and Air Heating Coils, 2000.
[22] H.J. Lee, J. Ryu, S.H. Lee, Influence of Perforated Fin on Flow Characteristics and Thermal Performance in Spiral Finned-Tube Heat Exchanger, Energies 12 (3) (2019) 556.